Regenerative Engineering and Translational Medicine (2023) 9:263–278
https://doi.org/10.1007/s40883-022-00281-y

ORIGINAL RESEARCH

Effect of Therapeutic Ultrasound on the Mechanical and Biological Properties of Fibroblasts

Rosy P. Cárdenas-Sandoval[1,2] · Homero F. Pastrana-Rendón[3,4] · Alba Avila[3] · Angélica M. Ramírez-Martínez[5] · Myriam L. Navarrete-Jimenez[6] · Alejandro O. Ondo-Mendez[7] · Diego A. Garzón-Alvarado[2,8]

Received: 15 February 2022 / Revised: 24 August 2022 / Accepted: 1 October 2022 / Published online: 28 November 2022

Abstract

Purpose This paper explores the effect of therapeutic ultrasound on the mechanical and biological properties of ligament fibroblasts.

Methods and Results We assessed pulsed ultrasound doses of 1.0 and 2.0 W/cm^2 at 1 MHz frequency for five days on ligament fibroblasts using a multidisciplinary approach. Atomic force microscopy showed a decrease in cell elastic modulus for both doses, but the treated cells were still viable based on flow cytometry. Finite element method analysis exhibited visible cytoskeleton displacements and decreased harmonics in treated cells. Colorimetric assay revealed increased cell proliferation, while scratch assay showed increased migration at a low dose. Enzyme-linked immunoassay detected increased collagen and fibronectin at a high dose, and immunofluorescence imaging technique visualized β-actin expression for both treatments.

Conclusion Both doses of ultrasound altered the fibroblast mechanical properties due to cytoskeletal reorganization and enhanced the regenerative and remodeling stages of cell repair.

Lay Summary Knee ligament injuries are a lesion of the musculoskeletal system frequently diagnosed in active and sedentary lifestyles in young and older populations. Therapeutic ultrasound is a rehabilitation strategy that may lead to the regenerative and remodeling of ligament wound healing. This research demonstrated that pulsed therapeutic ultrasound applied for 5 days reorganized the ligament fibroblasts structure to increase the cell proliferation and migration at a low dose and to increase the releasing proteins that give the stiffness of the healed ligament at a high dose.

Future Works Future research should further develop and confirm that therapeutic ultrasound may improve the regenerative and remodeling stages of the ligament healing process applied in clinical trials in active and sedentary lifestyles in young and older populations.

Keywords Ultrasonic therapy · Cell proliferation · Cell movement · Elastic modulus · Cytoskeleton

✉ Rosy P. Cárdenas-Sandoval
rosy.cardenas@urosario.edu.co

[1] Rehabilitation Science Research Group, School of Medicine and Health Sciences, Universidad del Rosario, 111221 Bogotá, Colombia

[2] Organ and Tissue Mechanobiology Research Group. Biotechnology Institute, Universidad Nacional de Colombia, 111321 Bogotá, Colombia

[3] Microelectronics Center (CMUA), Department of Electrical and Electronic Engineering, Universidad de los Andes, 111711 Bogotá, Colombia

[4] Doctorado en Ciencias de La Salud, Universidad Antonio Nariño, 111821 Bogotá, Colombia

[5] Department of Biomedical Engineering, Universidad Militar Nueva Granada, Campus, 250247 Cajicá, Colombia

[6] Department of Microbiology, Faculty of Medicine, Universidad Nacional de Colombia, 111321 Bogotá, Colombia

[7] Clinical Research Group, School of Medicine and Health Sciences, Universidad del Rosario, 111221 Bogotá, Colombia

[8] Department of Mechanical and Mechatronics Engineering, Universidad Nacional de Colombia Bogotá, 111321 Bogotá, Colombia

Introduction

Therapeutic ultrasound produces sound waves to create vibrations that exert forces on cells and stimulate the regenerative and remodeling stages coordinated by fibroblasts during the wound healing process [1–3]. Nevertheless, the exact doses of ultrasound that may affect the ligament fibroblast elastic modulus and harmonic vibration to improve the regenerative and remodeling stages remain largely elusive. The elastic modulus of cells is a biomarker that determines several biological responses such as communication with the environment, cell death, aging, and cellular motility [4–6]. It may also influence the harmonic vibration (i.e., natural vibration frequencies of the cell structure) [7], which is the rate at which the structure oscillates at a point of balance without being affected by an external force [8].

Therapeutic ultrasound generates a micro-massaging effect caused by compression and negative pressure from micro-vibration and cavitation [9–13]. Cellular transmembrane receptors such as integrins and cadherins detect these forces. Consequently, external stimuli are conducted rapidly along cytoskeleton filaments and absorbed at reserved edges in the cytoplasm and nucleus, modifying the cellular genome activities by increasing collagen synthesis and activating the mitotic activity of cells [14–16].

Cells react to external physical stimuli caused by ultrasound by altering their cytoskeleton, which is the structure responsible for regulating the mechanical behavior of cells. The cytoskeleton maintains the cell shape, responds to external mechanical cues, exerts forces, and produces motion [13, 17, 18]. In addition, it transduces the mechanical signal and converts it into a biological response associated with the wound healing process. This mechanotransduction process is evidenced by measuring changes in the mechanical properties of cells [4–6, 17, 19–22].

The mechanical and biological effects of conventional ultrasound doses of 0.1–3 W/cm^2 spatial average temporal average intensity (SATA) at 1–3 MHz frequency to ligament fibroblasts remain unclear [23]. The evidence so far has shown contradictory results: On the one hand, when therapeutic ultrasound is applied at conventional frequencies [9–12], there is no resonance effect; in other words, cell harmonics differ from ultrasound frequency. For example, when using therapeutic ultrasound at 1 MHz and low intensities (less than 1.0 W/cm^2), ultrasound improves cell proliferation and extracellular matrix (ECM) [20, 23–26] and cell migration [24] by modulating cell cytoskeleton organization [20, 25].

On the other hand, when applying ultrasound at low frequencies in the kHz range, typically, a resonance effect occurs, compromising cell structure integrity because of the oscillation at such frequencies that coincide with the harmonic vibration of the cell [7, 26–28]. For instance, when applying ultrasound at frequencies between 550 and 650 kHz, cell death increases, and cell proliferation decreases in breast cancer cells [29].

The effects of conventional doses of therapeutic ultrasound used in rehabilitation [23] on the elastic modulus and harmonic vibration (mechanical properties), as well as on the viability, proliferation, migration, and synthesis of the ECM (type I collagen, type III collagen, and fibronectin) and β-actin expression (biological properties) of ligament fibroblasts in joints remain uncertain [30–34]. The controversy concerning the contradictory results of ultrasound and the lack of evidence motivated us to measure and demonstrate that conventional doses of therapeutic ultrasound can modulate the mechanical and biological properties by the ligament fibroblast cytoskeleton reorganization to improve the cell functions associated with wound healing.

Therapeutic ultrasound modifies the elastic modulus of cells and their harmonic vibration, while cells reorganize their cytoskeleton structure without resonance or harmful effects. It also improves the regenerative and remodeling functions of ligament fibroblasts. However, clinicians cannot evaluate this complex effect by patient assessment. Thus, we applied a multidisciplinary approach that integrates in vitro and computational techniques to assess the impact on the mechanical and biological responses of ligament fibroblasts of joints by using two intensities of conventional pulsed therapeutic ultrasound, namely, a low dose of 1.0 W/cm^2 and a high dose of 2.0 W/cm^2, both at a frequency of 1 MHz applied for 5 days. Furthermore, we determined the specific ultrasound dose required to improve the regenerative (cell proliferation and migration) and remodeling (extracellular matrix synthesis) of the ligament fibroblast healing process.

Materials and Methods

We show the summary methods in Fig. 1. For additional details of conventional procedures to evaluate the biological properties of ligament fibroblasts, refer to the supporting information (S1 File).

Ligament Fibroblast Explant

An explant technique allowed ligament fibroblasts' obtention. Lateral Collateral Ligaments (LCLs) came from two male Wistar rats sacrificed from the animal research facility of the Pharmacy Faculty. They were sacrificed for exhibiting aggressive behavior. According to international regulations for laboratory animals, a zoologist specialist sacrificed the Wistar rats by using a faster CO_2 euthanasia method

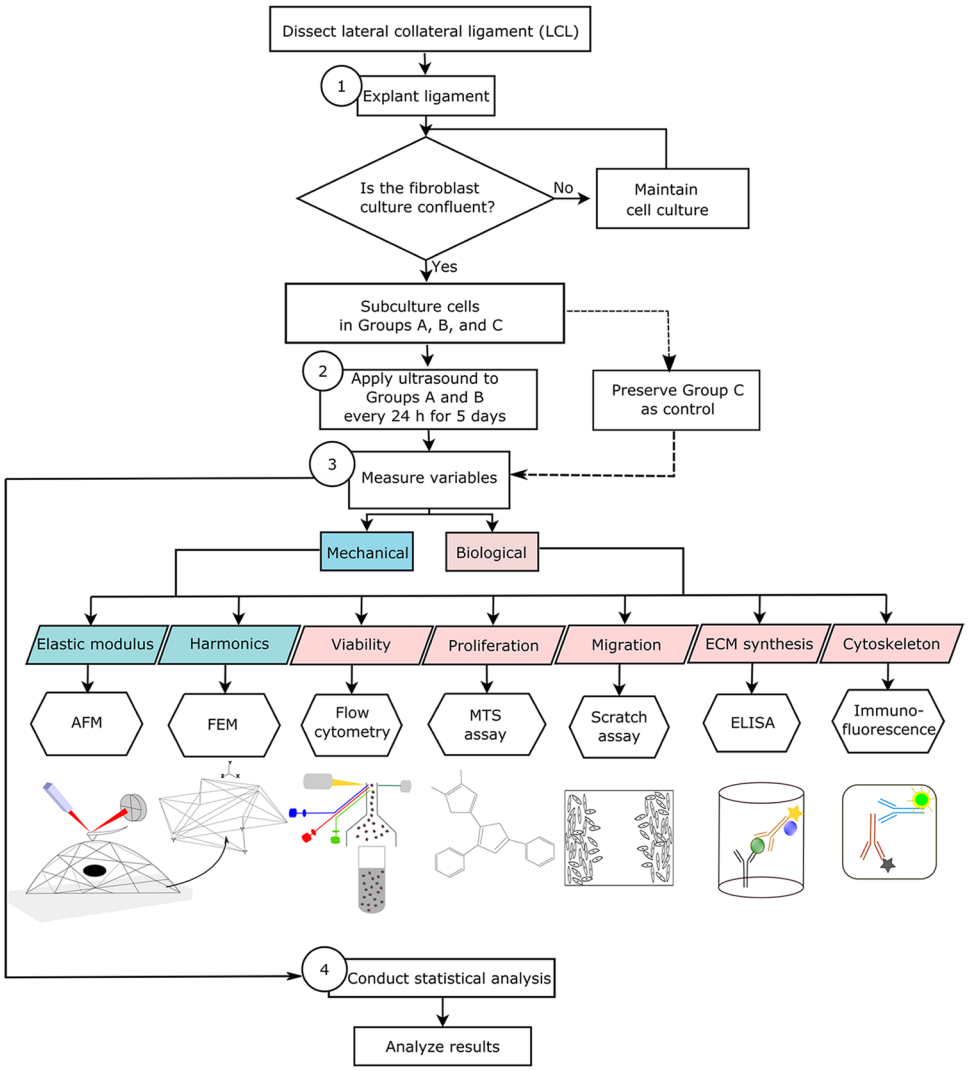

Fig. 1 Summary methods. (1) Ligament explant, (2) ultrasound stimulation, (3) measurement of mechanical and biological parameters, and (4) statistical analysis

to decrease distress time. Then, an anesthetic protocol was unnecessary. After the research was complete, it was not necessary to sacrifice other rats. Finally, the ethics committee of the Faculty of Sciences at the Universidad Nacional de Colombia (Protocol Number: FC-13–01,082,016) approved the research protocols.

First, dissection of LCLs was performed with a scalpel to cut the femoral and fibular insertions. Then, we placed the LCLs into T-25 culture flasks containing a sterile supplemented culture medium (Fig. 2A–C). The only modification we made to the explant technique proposed by Henshaw et al. was using a different culture medium [35]. Then, we maintained the explant pieces of LCL under aseptic conditions in a 1:1 mixture of Dulbecco's modified Eagle medium and nutrient mixture F-12 (DMEM/F12; DF-041-B; Merck Millipore) supplemented with 1% antibiotic/antifungal (15,240,062; Gibco) and 10% fetal bovine serum (FBS; 12,657,029; Gibco). Next, the culture medium was changed every 48 h, and we incubated the flasks at 37 °C in a humidified atmosphere containing 5% CO_2.

Ligament cells were motile around the explanted tissue and then adhered to the flasks where they grew. To ensure that cells obtained from ligaments corresponded to fibroblasts, we followed the laboratory protocol described by Spitalnik [36], and we highlighted the cell nuclei and bodies using hematoxylin–eosin staining (H&E) and microscopic observation [37]. As a result, cells had an average and typical fibroblast shape, namely, adherence; the presence of nucleus and body; flat, elongated, and triangular shape; and linkage between cells, were evident [38] (Fig. 2D). After 15 days, the monolayer cultures became confluent, and we removed the tissues from the flasks.

Finally, we washed ligament fibroblast with Hank's balanced salt solution (14,065,056; Gibco), detached using 0.025% trypsin (15,400,054; Gibco) for 5 min, centrifuged at $287 \times g$ for 5 min, and subcultured for subsequent experiments. We cryopreserved the remaining cells in a mixture of 10% DMEM/F12, 80% FBS, and 10% dimethyl sulfoxide.

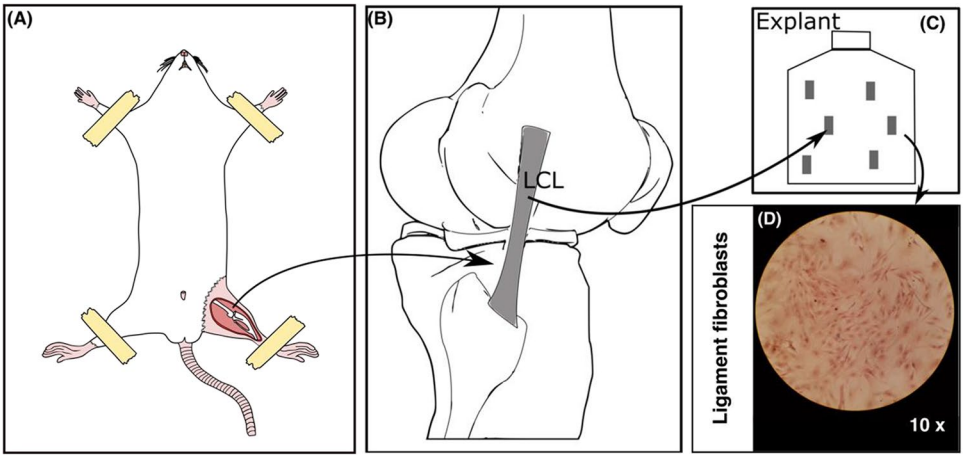

Fig. 2 Ligament fibroblast explant. **A** Adult male Wistar rat. **B** Lateral Collateral Ligament (LCL). **C** Small pieces of the ligament tissue cultured in a T-25 culture flask. **D** Verified and stained adherent ligament fibroblasts with H&E

Pulsed Ultrasound Intensity and Application Time

The protocol of ultrasound therapy applied to cultured cells followed the standard clinical guidelines for ligament treatment [39–42]. We applied pulsed ultrasound at 1 MHz of frequency 1:1 (1 ms on; 1 ms off), which means 50% of duty cycle every 24 h for 5 days to the two treatment groups we designed. Treatment Group A received 1.0 W/cm^2 (low dose), whereas treatment Group B received 2.0 W/cm^2 (high dose) of the maximum intensity and energies of 1.5 and 5.0 J/cm^2 for the low and high dose, respectively. We selected these energy values according to the dosage for in vitro studies, corresponding to 5% and 17% of the 30 J/cm^2 applied in human therapy [39–41, 43, 44]. The SATA values were 0.5 W/cm^2 and 1.0 W/cm^2 for the low and high doses. The ultrasound transducer showed an effective radiated area (ERA) of approximately 5.0 cm^2. We applied a different time according to the surface area of the well plate by using the potency equation of energy transmission [11, 12, 45] (see P1 and P2 Protocols).

Fibroblast Elastic Modulus by AFM

Fibroblasts (3.5×10^4 cells from each treatment group) were cultured in Petri dishes after 5 days of ultrasound treatment. If they reached 20–40% confluency on the 6th day, we measured the elastic modulus of viable cells maintained in DMEM/F12 within 2–3 h of the duration of the measurements. Then, we monitored changes in the cell elastic modulus using AFM (MFP3D-Bio AFM system, Asylum Research, Santa Barbara, CA) [46, 47].

We employed soft cantilevers T R400P B (Olympus, Japan) with a nominal spring constant of 0.09 N/m, a tip radius of 42 nm, and a half-opening angle of 35°. The relative trigger force was 2 nN. To estimate the elastic modulus, we used the force–volume technique by measuring the cantilever deflection as a function of the cell position. A video microscope allowed placing the AFM tip precisely over the cell surface. The probe moved up and down, simultaneously registering the force curve and cell topography at each surface pixel. As a result, we obtained force–volume images with a resolution of 20×20 pixels within 30×30 μm^2 scan areas for ten cells per group and a 15-min approximate acquisition time per image.

We performed 863, 866, and 338 indentations from ten cells for the high and low doses and the control group. A larger sample of indentations to calculate the average elastic modulus values avoided errors associated with the indentation depth. In addition, force curves determined from a relative area above the whole cell enabled the comparison of induced changes to a constant force. We calculated the elastic modulus using the Sneddon and the asymptotical correction model [48] as indicated in Eq. 1:

$$F_e = \frac{8}{3}\frac{E}{\pi}tan(\theta)\delta^2\left\{1 + C\frac{4}{\pi^2}\frac{\delta}{h} + C^2\frac{20}{\pi^4}\frac{\delta^2}{h^2} + 0\left(\frac{\delta^3}{h^3}\right)\right\} \quad (1)$$

Here, F_e is the elastic force, E is the elastic modulus, δ is the indentation depth, θ is the rigid cone angle (set as 35°), h is the thickness of adherent cells at the point of indentation (set as 150 nm), 0 represents higher-order terms in the series (assumed to be negligible), and $C = 1.7795\tan(\theta)$ [48]. For additional details of the parameters used in the asymptotical correction model, refer to supporting information (S2 File).

Harmonic Vibration and Modal Analysis by Finite Element Method (FEM)

We proposed a simplified theoretical model to consider only the cytoskeleton, as it predominantly determines cell mechanics and its response to external stimuli [49, 50]. A three-dimensional (3D) octahedron tensegrity model with 12 coordinates and 30 beam elements represented the ligament fibroblast cytoskeleton elements

(actin filaments, intermediate filaments, and microtubules) (Fig. 3) [51]. Then, the FEM analysis predicted the 50th natural vibration frequencies (harmonics) and eigenforms of the ligament fibroblast cytoskeleton using the eigenvalue extraction method Lanczos (ABAQUS/CAE 6.12.3 software). Refer to the supporting information (S3 File) for additional details.

We used the elastic modulus median and the mean height values for the treatment groups and the control group from the AFM results as input parameters for the tensegrity structure to calculate the harmonic vibration and perform the modal analysis for every cytoskeleton configuration in each group [46, 52]. In addition, we used the data for the Poisson's ratio, length, and beam radius of the tensegrity structure from the literature. These values are provided in Table 1 [53–56].

While cells exhibited small deformations of 2–8%, we considered cytoskeleton filaments (beam elements) isotropic and elastic [56–59]. In the simulation, we converted the material properties units to microscale. The beam length of the contact radius in the tensegrity structure was 11.2 µm [56]. The filament density was 1.15×10^{-6} µg/µm^3 [7]. We configurated the initial boundary conditions on the three base nodes of the tensegrity structure [56]. These three base nodes represented the focal adhesion of the cell receptors to the ECM because ligament fibroblasts are adherent cells and are dependent on the actin cytoskeleton [60]. They were constrained for three degrees of freedom (U1 = U2 = U3 = UR1 = UR2 = UR3 = 0).

We used the height values (Y axes) for each octahedron structure from the mean values obtained in the AFM force–volume topography maps and the *X* and *Z* axes from the literature to comply with the spread shape of an adherent cell [56, 61].

Statistical Analyses

We conducted the statistical analyses using BioVinci software version 2.8.5 for Windows (BioTuring Inc., San Diego, California, USA, www.bioturing.com). All data were representatives of at least two independent experiments. First, we assessed normality using the Shapiro–Wilk test, Pearson chi-square test, one-sample Kolmogorov–Smirnov test, and Jarque–Bera test. Because the data distribution was not normal, the medians (elastic modulus, harmonics, cell proliferation and migration, ECM synthesis, and β-actin shortening area) were compared across groups using a nonparametric multiple comparison Kruskal–Wallis test. The data were presented as a boxplot with medians for elastic modulus, harmonics, and ECM synthesis, and standard errors of the means (SEMs) for the cell proliferation, cell migration, and β-actin shortening area. We assumed statistical significance at $P < 0.05$.

Results

Effect of Ultrasound Treatment on Ligament Fibroblast Structure

The AFM revealed that the median elastic modulus of the treated ligament fibroblasts decreased by 22% for the low dose (1.0 W/cm^2) and 31% for the high dose (2.0 W/cm^2) compared to that of the control group. We found significant differences among the groups (***$P = 0.00001 \times 10^{-6}$; Fig. 4A). Moreover, the ligament fibroblast topography through 3D force–volume maps showed darker areas (decreased elastic modulus) and greater height for the treatment groups than for the control group (Fig. 4B). We highlight those darker areas corresponding to the

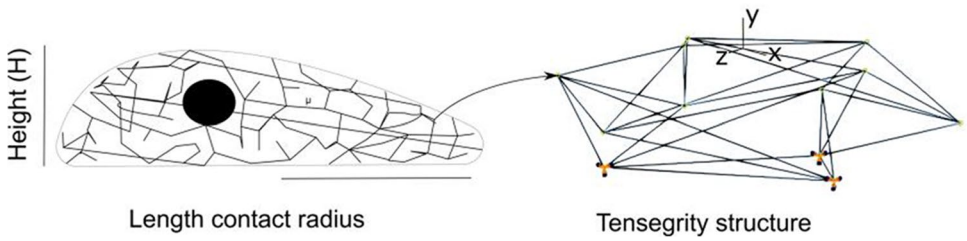

Fig. 3 Three-dimensional octahedron tensegrity model. Tensegrity structure represented the cell cytoskeleton geometry

Table 1 The cytoskeleton material properties for the low and high doses and the control group

Material properties	Low dose 1.0 W/cm^2	High dose 2.0 W/cm^2	Control 0.0 W/cm^2	Reference
Elastic modulus (Pa)	1085 Pa	970 Pa	1399 Pa	Taken from the AFM results
Height (µm)	4.6 µm	3.1 µm	2.7 µm	Taken from the AFM results
Poisson's ratio (dimensionless)	0.4 ± 0.08	0.5 ± 0.05	0.36 ± 0.06	[7, 56]
Beam radius (m)	2×10^{-9} m	5×10^{-6} m	8×10^{-9} m	[55, 56]

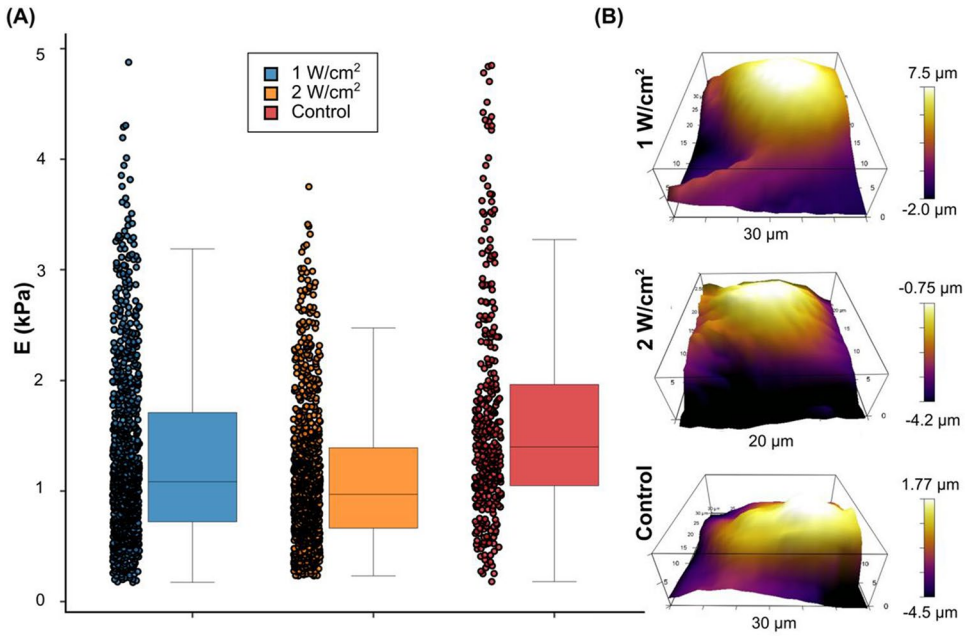

Fig. 4 Softening of ligament fibroblast structure due to low and high doses of ultrasound. **A** Boxplot showing medians with whiskers from minimum to maximum values. Each dot represents a measurement of the indentation. **B** 3D force–volume topography maps from AFM results

cell cytoskeleton zone and lighter areas matching the cell nucleus.

Effect of Ultrasound Treatment on Harmonic Vibration

The FEM predicted the natural vibration frequency for each cytoskeleton structure until the 50th harmonic and eigenform (mode of vibration). Ligament fibroblast cytoskeleton for the treated cells obtained similar displacements, but they were different compared to the control group, as shown in Fig. 5A in the 5th mode of vibration. Refer to the supporting information (S4 Movie A-C) for additional predicted vibration modes and displacements for each group. Regarding the natural vibration frequencies, a higher cytoskeleton filament elastic modulus (control group) produces higher frequencies, reaching a maximum vibration frequency of 4.1×10^9 Hz in the 50th vibration mode.

On the other hand, when the cytoskeleton filaments had the elastic modulus of treatment Groups A and B from the AFM results, the vibration frequencies decreased up to a maximum of 3.3×10^9 Hz in the 50th vibration mode for both structures (Fig. 5B). Additionally, the median of the 50th harmonic of natural vibration frequencies of the treated ligament fibroblasts decreased by 13% for the low dose (1.0 W/cm^2) and 17% for the high dose (2.0 W/cm^2) compared to that of the control group. Nevertheless, there was no statistically significant difference among the groups ($P = 0.514$).

Effect of Ultrasound Treatment on the Viability of Ligament Fibroblasts

Histograms from the cell death assays indicated the number of cells stained with Annexin V-FITC and PI (Fig. 6A). Flow cytometry showed that most cells were viable in the treatment and control groups (Fig. 6B). The number of events collected was 10,000. The results showed that cell viability slightly decreased by 1% for the low dose (1.0 W/cm^2) and 10% for the high dose (2.0 W/cm^2) compared to the control group. In addition, all groups have a small percentage of ligament fibroblasts in necrotic (Quartile 1) and late apoptosis (Quartile 2). However, the high dose produced the lowest percentage of viable cells (Quartile 3) and the highest

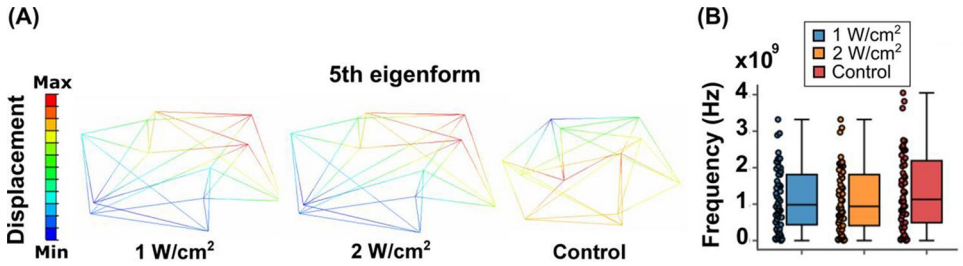

Fig. 5 Alteration of ligament fibroblast cytoskeleton due to ultrasound treatment. **A** 3D tensegrity structure for ligament fibroblast cytoskeleton. **B** Boxplot showing medians with whiskers from minimum to maximum values

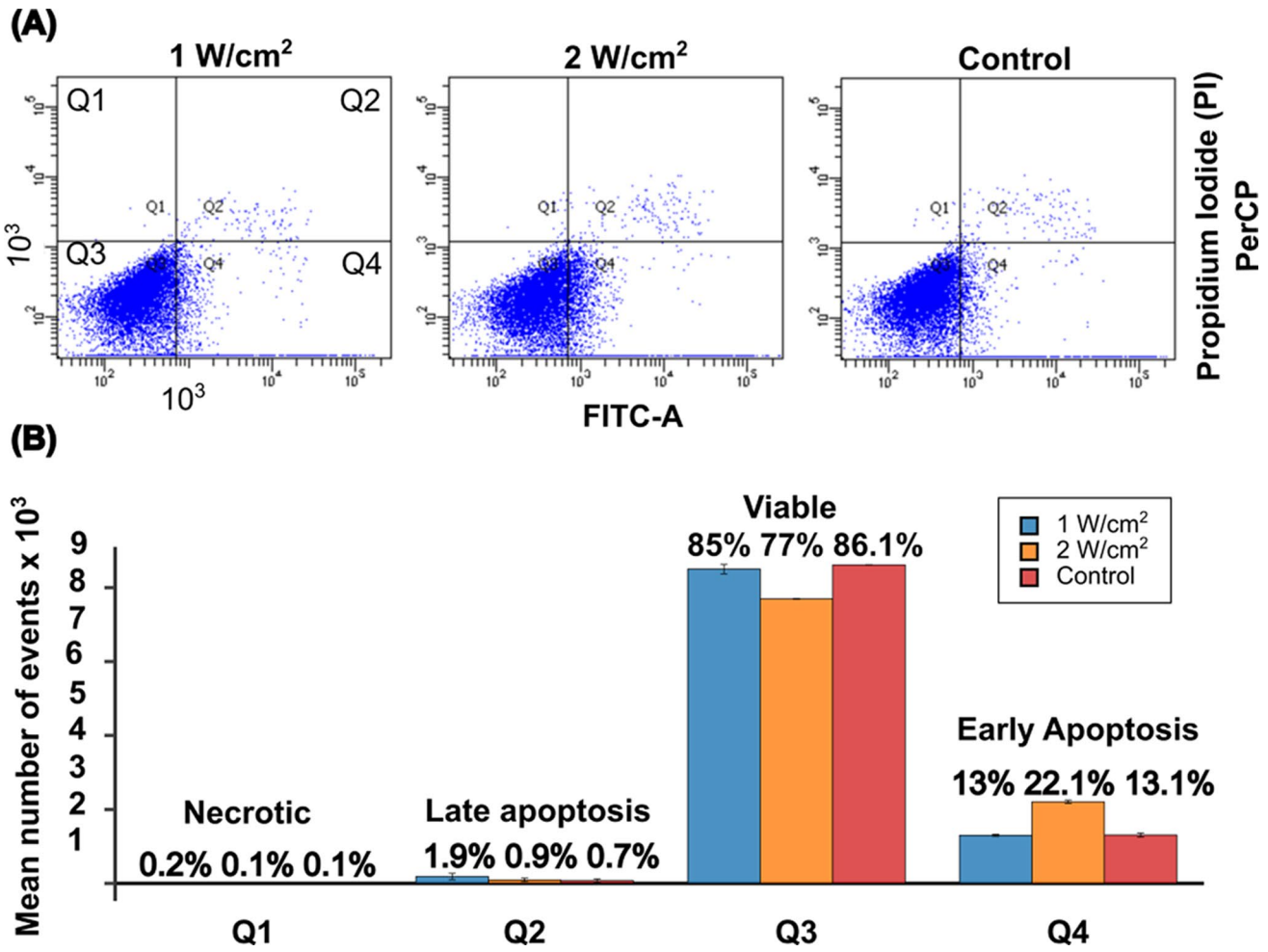

Fig. 6 Negligible effect of low and high doses of ultrasound on the viability of ligament fibroblasts. **A** Histogram and dot plot of cell viability assay using Annexin V-FITC and cationic marker PI. Quartile 1, necrotic cells; Q2, late apoptotic cells; Q3, viable cells; and Q4, early apoptotic cells. **B** Bar plot of the mean number of events for each quartile of the flow cytometry data

percentage of cells in early apoptosis (Quartile 4) among the groups (Fig. 6A and 6B).

Effect of Ultrasound on Fibroblast Cell Proliferation and Cell Migration in the Regenerative Stage

We used the MTS assay to determine the cell number in proliferation for the treatment groups and the control group during ultrasound stimulation for 5 days (1st and 3rd days) and 24 h after treatment (6th day) by measuring the mitochondrial activity. We observed a typical growth curve for all groups when comparing the mean cell density for the 1st day of treatment to the 6th day post-treatment. However, cell density showed a slightly fluctuating percentage of change, for example, 90% of cell proliferation at the low dose (1.0 W/cm^2), 91% at the high dose (2.0 W/cm^2), and 92% for the control group.

Subsequently, on the 1st day of culture, the mean cell density increased by 25% for the low dose and decreased by 11% for the high dose compared to that of the control group. The 3rd day of culture decreased by 11% and 9%, respectively. Finally, on the 6th day of culture (1st post-treatment day), it increased 10% at the low dose but decreased 13% at the high dose. We found significant differences among the groups ($*P = 0.041$; Fig. 7A) post-treatment. Results were obtained and analyzed for 18 samples.

Afterward, the scratch assay assessed the cell migration for the treatment groups and the control group after ultrasound stimulation for 5 days. The assay showed that the mean migration length of ligament fibroblasts increased by 4% for the low dose and decreased by 11% for the high dose compared to that of the control group after treatment (6th day). We found significant differences among the groups ($***P = 0.00003 \times 10^{-4}$; Fig. 7B). The image analysis produced 102 images for each treatment group and 107 for the

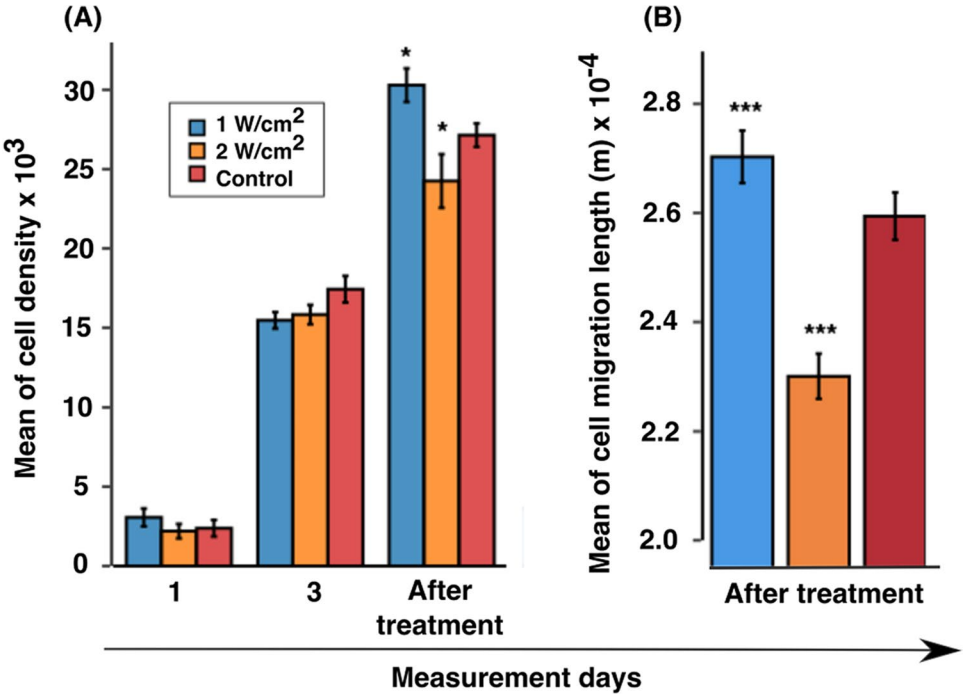

Fig. 7 An increase in fibroblast cell proliferation and cell migration in the regenerative stage due to the low dose of ultrasound applied for 5 days. **A** The mean cell number in proliferation and **B** the mean migration length (μm) of ligament fibroblasts is higher for the low dose on the 6th day after treatment. Error bars indicate SEMs

control groups. We analyzed 494 displacement measurements from the treatment group at the low dose, 613 from the treatment group at the high dose, and 641 from the control group. We excluded twenty images from the low dose group because of their poor quality. In general, we observed in common that ligament fibroblasts increased proliferation and migration at the low dose.

Effect of Therapeutic Ultrasound on the Protein of ECM: Type I Collagen, Type III Collagen, and Fibronectin Synthesis in the Remodeling Stage

On the 6th day post-treatment, both treatment groups and the control group did not express enough type I collagen or type III collagen protein despite the absorbance measurement of the OD being higher than zero. Refer to the supporting information for additional details (S5 File). Thus, after constructing the curvilinear regression line using the standard, these OD values were lower than the minimum of the standard curve, which indicates no detected protein concentrations (ng/mL) as shown in Fig. 8; although fibronectin was increased by 79% for the low dose, it was not enough expressed for the high dose regardless of the OD values higher than zero. In contrast, compared to the control group, on the 10th day after the stimulation period, the low dose of ultrasound increased the concentration of both collagens (type I collagen by 30%; type III collagen by 33%) but decreased fibronectin by 33%. Furthermore, compared to the control group on the 10th day after the stimulation period, the high dose of ultrasound increased the concentration of

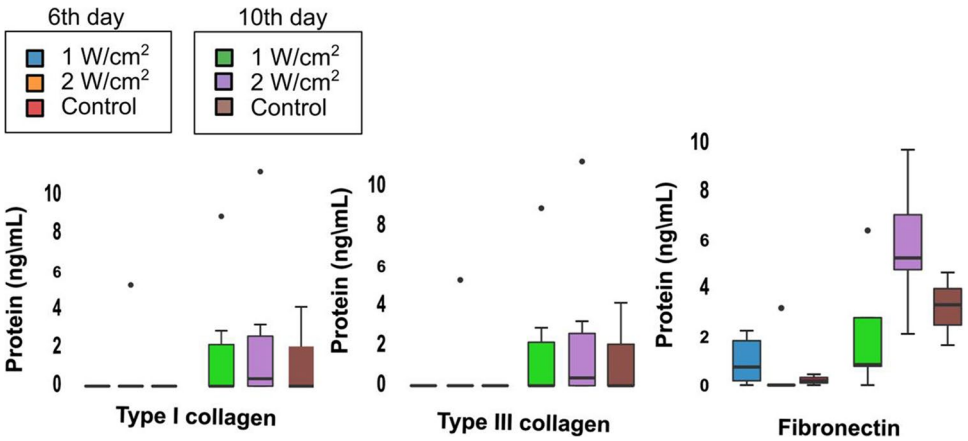

Fig. 8 Increase in ECM concentration in the remodeling stage due to therapeutic ultrasound. Protein concentration in cell culture supernatants of ligament fibroblasts. The ELISA assay measured protein concentration for type I collagen, type III collagen, and fibronectin after ultrasound treatment (on the 6th of evaluation) and on the 10th day of re-evaluation

the three proteins: type I collagen by 45%; type III collagen by 71%; and fibronectin by 44%. A box plot shows the protein concentration data, including at least five averaged measurements (Fig. 8).

Effect of Therapeutic Ultrasound on β-Actin Expression for Promoting Regenerative and Remodeling Stages

Immunofluorescence imaging detected β-actin (an essential structural protein of the cell cytoskeleton) in both treated and control ligament fibroblasts. Previously, we found that both doses of therapeutic ultrasound decreased the elastic modulus of ligament fibroblasts, an effect caused by cytoskeleton reorganization, which was confirmed for both treatments in our images through β-actin expression represented by the green cell area in Fig. 9A.

Interestingly, the immunohistochemistry image analysis showed a greater β-actin shortening area in the treatment groups (Fig. 9B). Although there was no statistically significant difference among the groups ($P = 0.373$), compared to the control group, after the stimulation period, the low dose of ultrasound increased the mean of the β-actin shortening area by 71%, and the high dose by 25%. In addition, compared to the high dose after the stimulation period, the low dose of ultrasound increased the mean of the β-actin shortening area by 62%.

It should be noted that results were obtained and analyzed for three different samples. Refer to the supporting information (S6 File) for additional details.

Discussion

Our results demonstrated that low and high doses of pulsed therapeutic ultrasound applied at 1 MHz for 5 days modify the mechanical and biological properties of ligament fibroblasts. Figure 10 integrates the results of this study.

Regarding the mechanical properties, we proved that ligament fibroblasts treated with low and high doses of pulsed therapeutic ultrasound tend to be softeners than the control group [62] but possess the strength to maintain the cell shape without rupture. In other words, the resistance required to deform the ligament fibroblast with the AFM tip was lower for the treatment groups, as shown in Fig. 4A. Therefore, the ligament fibroblast elastic modulus is dependent on ultrasound stimulation. Furthermore, while the cell elastic modulus measured by AFM may elucidate the changes in cytoskeleton elasticity [46, 52], we infer that ultrasound stimulation produces cytoskeleton reorganization, as we verified by cytoskeletal displacements observed in treated cells (Fig. 5A) and shortening of the β-actin area (Fig. 9).

Our results are comparable to those of previous studies on cancer cells. Low-intensity pulsed ultrasound stimulation at 20 kHz of frequency and energies between 2.8 and 6.6 J/cm^2 also decreased the cell elastic modulus for squamous cells, carcinomas, and melanomas, indicating that cancer cells were less stiff than noncancerous cells [63].

In epithelial and endothelial cell lines derived from human breast cancer (MCF-7) compared to human umbilical vein endothelial cells (HUVEC), low-intensity ultrasound stimulation for 2 s with a frequency of 20 kHz, applied at two intensities of 0.9 and 1.8 W/cm^2, produced a lower elastic modulus caused by less organized and decreased actin fibers of the cytoskeleton [13].

Therefore, as the dosage of ultrasound decreases the stiffness of cancer cells, it also decreases the elastic modulus of ligament fibroblasts. A study found a strong relationship between ultrasound frequency and the elastic modulus of breast cancer cells. For example, at a frequency of 450 kHz and 60-s exposure to ultrasound, the cell elastic modulus initially tended to increase by 50%. However, when the frequencies were 550–620 kHz, the cell elastic modulus decreased by 50% [29]. Therefore, we suggest that the higher frequency used in our study at 1.0 MHz on ligament fibroblasts may influence the cytoskeletal deformation and, consequently, a decreased elastic modulus.

Although our experimental elastic modulus (Fig. 4A) showed greater dispersion for ligament fibroblasts, the median values were in the range of NIH3T3 fibroblasts

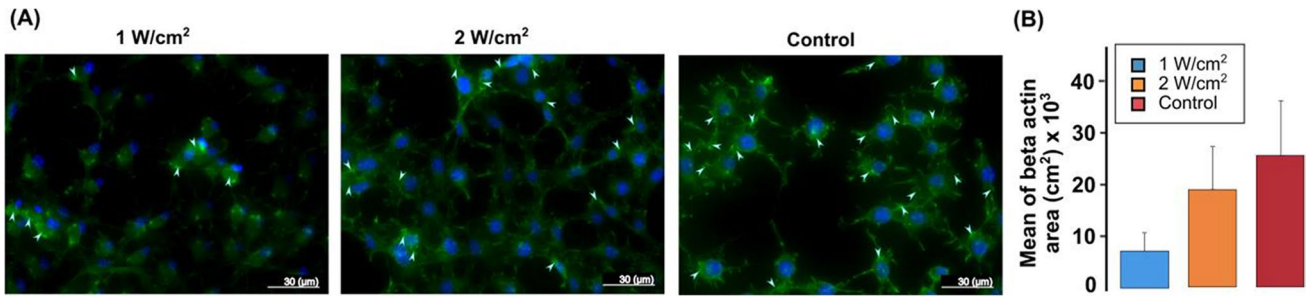

Fig. 9 Alteration of β-actin expression to promote the regenerative and remodeling stages due to therapeutic ultrasound. **A** Immunofluorescence analysis of β-actin (green) and cell nuclei (blue) in ligament fibroblasts. **B** Mean of β-actin shortening area (cm^2). Error bars indicate SEMs

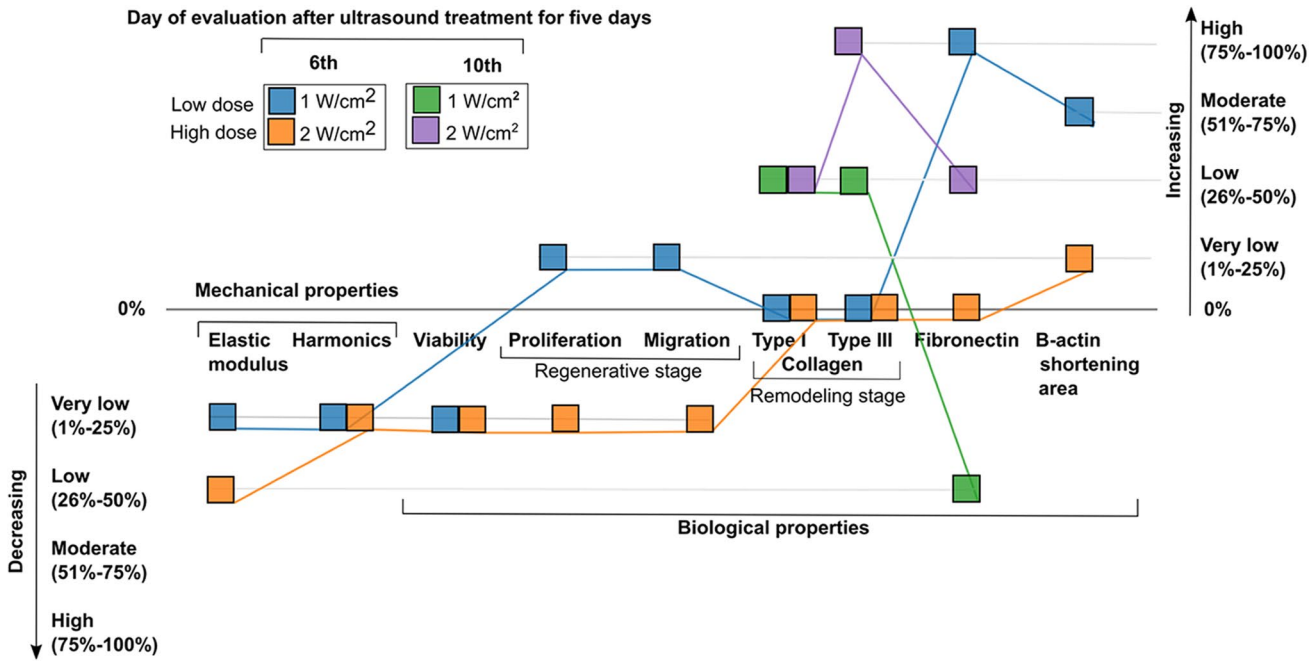

Fig. 10 Low and high doses of pulsed therapeutic ultrasound applied for 5 days alter the mechanical and biological properties of ligament fibroblasts. This study evaluated all variables after treatment on the 6th day and re-evaluated the ECM proteins on the 10th day

and noncancerous cells (0.8–5 kPa) [13, 62, 64]. The AFM indentation random procedure may influence this dispersion in the elastic modulus, which can include one or more of the following: cytoskeleton, membrane, and cell organelles.

Because the elastic modulus obtained by using the rigid cone indenting and computed by the Sneddon model may create a bottom substrate effect, a typical error found in adherent cells where their elastic modulus seems stiffer [65], we used an asymptotical correction model to nullify this source of error [48] (see supporting information (S2 File)). In addition, although stiffer substrates may increase the cell elastic modulus and decrease cellular height and cell migration [29], only the control group showed a higher elastic modulus. It means that therapeutic ultrasound is the primary source that alters the mechanical properties of ligament fibroblasts more than the stiffness of the surrounding location.

Concerning the decrease in the elastic modulus of both treatment groups, we predicted the natural frequencies of vibration of ligament fibroblasts cytoskeleton by using FEM analysis to detect a possible resonance effect with the ultrasound frequency. The simulation showed decreased harmonics and varied displacements for cytoskeleton for both treatment groups. Then, while the AFM results characterized the cytoskeleton structure in the FEM analysis, we confirmed that vibration modes and harmonics depended on the elastic modulus decreased by ultrasound stimulation [7].

Although FEM results showed no significant differences between groups for the 50th harmonic frequencies predicted, we validated that harmonics for the cytoskeleton in the control group were higher than in the treatment groups (Fig. 5B), such as in normal cells owing to their high elastic modulus [7, 66]. Moreover, to resist the external forces due to the mechanical stimulation produced by ultrasound [17, 18], the cytoskeleton structure is deformed through different displacements observed in each mode of harmonics between the treatment and control groups (Fig. 5A) [7].

While our goal was to analyze only cytoskeleton dynamics, since it mainly provides the cell structure, balance, and resistance against external forces, we excluded the cytoplasm and nucleus from our simulation [14–17]. This simplified geometry configuration may explain why the values of natural vibration frequencies that we reported (3.3×10^9–4.1×10^9 Hz) vary from those obtained in previous studies ($21–34\times10^3$ Hz for tumor cells) [7, 66].

Accordingly, our results suggest that pulsed therapeutic ultrasound applied at 1 MHz induces a low risk of cell damage by the resonance effect since the frequency values for the cytoskeleton harmonics differed from the ultrasound frequency [9–12]. We also confirmed that therapeutic ultrasound does not induce harmful effects due to an unstable cavitation threshold, that is, expanding bubbles originating in a liquid collapse severely, causing damage to the nearest structure [32, 67]. The absence of a resonance effect and cavitation consequence may explain why cell viability did not change by more than 1% and 10% for the low and high doses, respectively.

In addition, ligament fibroblasts do not perceive the treatments as negative stimulation because their cell

death and early apoptosis levels are comparable to those of the control group cells (Fig. 6). Lucas et al. supported these results, demonstrating that low and high doses of ultrasound stimulation are safe and do not affect cell viability or apoptosis [23]. However, the high-dose group had the greatest late apoptosis [23, 73]. This finding may be related to the amount of reflection that might produce higher doses of ultrasound [68]. Ivon et al. showed similar effects on myelomonocytic lymphoma cells, where low-intensity ultrasound stimulation for 90 and 180 s with a frequency between 400 and 620 kHz applied at two intensities of 0.045 and 0.09 W/cm^2 after 6 h produced a low percentage of early apoptosis; in contrast, they found lowest late apoptosis and decreased cell proliferation [69].

In nasopharyngeal carcinoma cells, continuous low-intensity ultrasound with 1.35 W/cm^2 spatial average intensity at a frequency of 1.7 MHz produced cytotoxic effects after 18 h of ultrasound stimulation. Specifically, Wang et al. observed autophagy, apoptosis, and mitochondrial structural and functional damage to cancer cells [70]. Bergman et al. also demonstrated that the viability decreased in cancer cells due to a lesser frequency applied in ultrasound (20 kHz) [63].

These studies suggest that every cell responds differently to the ultrasound stimulation dosages and the modality (pulsed or continuous) of application. Then, prolonged continuous ultrasound stimulation at a high dose and frequencies near kilohertz produces a heating effect that may affect cell integrity [31, 71], and pulsed treatment at low or high intensities with kilohertz or megahertz of frequency generates a mechanical effect that may positively alter the cell functions while maintaining its viability [25, 72]. These reasons justified the dosage prescribed in our study: pulsed mode (50% duty cycle), low (1.0 W/cm^2) and high (2.0 W/cm^2) intensities, and short time of application of therapeutic stimulation at 1 MHz.

To this point, we confirmed the hypothesis that therapeutic ultrasound alters the mechanical properties of ligament fibroblasts by cytoskeleton reorganization without harmful effects. Then, the elastic modulus and harmonics are predictive biomarkers of ligament fibroblasts specialized biological functions related to the healing process, such as proliferation, migration, and formation of a new extracellular matrix [23, 71, 73–75].

For instance, first, we found that the low dose increased the proliferation and migration of ligament fibroblasts (Fig. 7) by using the MTS assay. It should be noted that our objective was to measure the changes in the cell density and not to calculate the rate of cell division after ultrasound stimulation [76]. Therefore, we interpret that a low dose of pulsed therapeutic ultrasound increases the metabolic activity of ligament fibroblasts during proliferation to improve the regenerative stage of ligament wound healing. Our results extend the previous findings where pulsed ultrasound increased fibroblast cell proliferation at 1.0 W/cm^2 [43, 77] and 0.2 W/cm^2 with 1 MHz of frequency [78].

Regarding cell migration, our results are consistent with previous studies on other mammalian cells. For example, Tsai et al. demonstrated that ultrasound at 1 MHz of frequency, 1.0 W/cm^2 of intensity, and a duty cycle of 20% enhances the migration of tendon cells without visible damage because of the mechanical effect of ultrasound [29]. Correspondingly, Man et al. reported that osteoblast cells exposed to the same frequency as in our study but, with low intensities (0.025 and 0.25 W/cm^2), exhibited increased cell migration by 40% [79]. In addition, low-dose ultrasound treatment enhanced the migration speed of osteoblasts (MC3T3) by 30% [80], relative migration by 150%, and proliferation by 80% in keratinocytes by activating signaling pathways [81].

Second, we observed contradictory results for the high-dose group. While the high dose diminished cell proliferation and migration after treatment, it increased the production of proteins in the ECM on the 10th day after stimulation compared to the other groups. Therefore, we infer that the high dose produces higher mechanical stimulation on ligament fibroblasts, and because of the mechanical signal transduction through the cytoskeleton, the cell increases collagen and fibronectin synthesis. Then, a high dose of pulsed ultrasound might improve the remodeling stage of the ligament healing process.

The complex processes of transcription, translation, and assembly implied in ligament fibroblasts to synthesize new proteins in the ECM may explain this increased time to observe the effect of ultrasound stimulation [82]. For these reasons, we re-evaluated the collagen synthesis on the 10th day (Fig. 8). Indeed, our findings regarding collagen synthesis on the 10th day after stimulation are consistent with other studies. For example, Tsai et al. found that pulsed (25%) low ultrasound intensities (0.1 and 1.0 W/cm^2) at 1 MHz stimulated the synthesis of type I and III collagen on tendon cells [83].

Lee et al. reported increased collagen type I at 20 kHz with high-intensity ultrasound (HIUS) treatment at 15% amplitude in the early time point and 10% and 12% amplitudes at the late time point on human dermal fibroblasts [84]. In general, the specific biological answer of cells depends on the dosage of ultrasound stimulation and cell type. In addition, compared to our findings, these studies commonly applied ultrasound at pulsed mode, producing a mechanical effect than heating.

Moreover, since cell-ECM adhesion alters cell shape, proliferation, and migration, we measured the synthesis

of fibronectin, a protein–ligand involved in the interaction between ECM proteins and transmembrane receptors [85]. Our results for the low dose after stimulation agree with those of Harle et al. They found that stimulation with lower ultrasound intensities (0.14–0.99 W/cm^2) in human osteoblasts upregulated fibronectin synthesis as in our study on the 6th day of evaluation [47]. Also, Lee et al. reported increased fibronectin at 20 kHz with high-intensity ultrasound (HIUS) treatment at 10%, 12%, and 15% amplitudes in the early and late time points related to the increased cell proliferation and migration as well in our study on the 6th day of evaluation for the low dose [84].

Alternatively, in human periodontal ligament cells, diminished fibronectin synthesis as in our study on the 10th day of evaluation for the low dose [43]. Therefore, we infer that fibronectin depends on the ultrasound dosage; however, simultaneous biological answers like proliferation and migration may regulate fibronectin and vice versa [84]. It explains a decreased fibronectin in the remodeling stage on the 10th day of evaluation for the low dose (Fig. 10).

Hence, we hypothesized that fibronectin initially increased to facilitate cell proliferation and migration (6th day of measurement) at the low dose. Then, it decreased due to a diminished necessity of ECM assembly considering a lesser synthesis of collagen than the high dose (10th day of measurement), as shown in Fig. 10. In the same way, we suggest that fibronectin initially decreased at the high dose due to more time required to assemble the ECM. Fibronectin increased at least 5 days after treatment (Fig. 10).

Our results showed that the synthesis of proteins depends not only on the stimulation dose but also on the number of days after stimulation, which indicates the importance of selecting the correct stimulation dose based on the regenerative and remodeling stages of the ligament healing process.

For example, we suggest applying a low dose to increase the proliferation and migration of ligament fibroblasts to the injured area during the regenerative stage of wound healing. In contrast, to increase the synthesis of type I and type III collagen in the remodeling of wound healing, we recommend applying a high dose of stimulation and evaluating the results on the 10th day after stimulation [21, 86].

Finally, we predicted that both doses of ultrasound increased the β-actin shortening area. Even so, it was more remarkable for the low dose. For this reason, we confirm that the ultrasound stimulation activates the cytoskeleton disassembly to allow the ligament fibroblasts functions to proliferate and migrate at the low dose [32, 87–89] and to facilitate collagen and fibronectin synthesis at the high dose. Furthermore, the decrease in the cell elastic modulus and harmonics and the varied cytoskeleton displacements verify the β-actin shortening area [87].

Atherton et al. support our results; they demonstrated that low intensity (0.3 W/cm^2) of pulsed ultrasound at 1.5 MHz activates pathways to diminish the cell adhesion to the ECM to allow cell migration through mechanosensitive focal adhesion and molecular regulators [88]. Furthermore, as shown in living fibroblasts, shortening of stress fibers occurs at the proximal end, reflected by a decrease in fluorescence intensity [89], as measured in our study (Fig. 9A). Nonetheless, to our knowledge, there is a lack of evidence about the effects of high doses of ultrasound on β-actin variations that verifies our findings [78].

To conclude, we confirm that low and high doses of pulsed therapeutic ultrasound on ligament fibroblasts produce a mechanotransduction process. The mechanical effect caused by ultrasound at 1 MHz is sensed by cells and transmitted by the cytoskeleton to activate gene expression. Consequently, ligament fibroblasts increased (i) cell proliferation and migration at the low dose and (ii) the generation of a new ECM at the high dose [90], diagnosed by decreased cell elastic modulus and harmonics and increased β-actin shortening area. Therefore, our results may help researchers justify the dosages of therapeutic ultrasound that can potentially improve the regenerative and remodeling stages of the ligament fibroblast healing process.

Conclusions

Using in vitro and computational methods, we demonstrated that pulsed therapeutic ultrasound at 1.0 MHz applied for five days at low (1 W/cm^2) and high (2 W/cm^2) doses decreased the elastic modulus and harmonics of ligament fibroblasts. The low dose improves cell proliferation and migration (regenerative stage), and the high dose enhances the proteins of extracellular matrix synthesis (remodeling stage). While both doses increase the β-actin shortening area, this confirms that therapeutic ultrasound produces a cytoskeleton reorganization, and the mechanical properties act as biomarkers to determine the specialized biological responses of ligament fibroblasts related to wound healing. We highlight that both doses of therapeutic ultrasound are safe and do not produce unstable cavitation or an unfavorable resonance effect.

Supplementary Information The online version contains supplementary material available at https://doi.org/10.1007/s40883-022-00281-y.

Acknowledgements We thank Ivan Bonilla for providing help with the collation data of fibroblast cells in proliferation and ECM synthesis experiments. In addition, we thank Edwin Gil, Juan Saiz, and Heber Castro for the collation and data measuring of the cell migration assay.

Author Contributions The contributions made by each author to the manuscript are presented in Table AC.

Table AC. Contributions made by each author to the manuscript.

	Elastic modulus	Harmonics	Cell viability	Cell proliferation	Cell migration	ECM synthesis	β-actin expression
Conceptualization	(CS), (PR), (AB), (RM), (GA)	(CS), (RM), (GA)	(CS)	(CS)	(CS), (OM)	(CS), (NJ)	(CS), (OM)
Data curation Formal analysis Investigation Methodology	(CS), (PR)	(CS), (RM), (GA)	(CS)	(CS)	(CS), (OM)	(CS), (NJ)	(CS), (OM)
Funding acquisition	(CS), (PR), (AB), (GA)	(CS), (GA)	(CS), (GA)	(CS), (GA)	(CS), (OM), (GA)	(CS), (NJ), (GA)	(CS), (OM), (GA)
Project administration	(CS), (GA)	(CS), (GA)	(CS), (GA)	(CS), (GA)	(CS), (GA)	(CS), (GA)	(CS), (GA)
Resources Software	(CS), (PR), (AB), (GA)	(CS), (GA)	(CS), (GA)	(CS), (GA)	(CS), (OM), (GA)	(CS), (NJ), (GA)	(CS), (OM), (GA)
Supervision	(AB), (GA), (RM)	(AB), (GA), (RM)	(AB), (GA)	(AB), (GA)	(AB), (GA), (OM)	(AB), (GA), (NJ)	(AB), (GA), (OM)
Validation	(CS), (PR), (AB), (RM), (GA)	(CS), (AB), (RM), (GA)	(AB), (GA)	(AB), (GA)	(AB), (GA), (OM)	(AB), (GA), (NJ)	(AB), (GA), (OM)
Visualization	(CS), (PR)	(CS), (RM), (GA)	(CS)	(CS)	(CS), (OM)	(CS), (NJ)	(CS), (OM)
Writing-original draft	(CS), (PR)	(CS)	(CS)	(CS)	(CS)	(CS)	(CS)
Writing-review and editing	(AB), (GA), (RM)	(CS), (AB), (RM), (GA)	(CS), (OM), (AB), (GA)	(CS), (OM), (AB), (GA)	(CS), (OM), (AB), (GA)	(CS), (NJ), (AB), (GA)	(CS), (OM), (AB), (GA)

Author A: Cárdenas-Sandoval (CS).
Author B: Pastrana-Rendón (PR).
Author C: Ávila-Bernal (AB).
Author D: Ramírez-Martínez (RM).
Author E: Navarrete-Jimenez (NJ).
Author F: Ondo-Mendez (OM).
Author G: Garzón-Alvarado (GA).

Funding Open Access funding provided by Colombia Consortium. This project was funded by DIB-Universidad Nacional de Colombia-2014, COLCIENCIAS (Colombia) Grant 712–2015, Scholarship Francisco Jose de Caldas # 567, and COLCIENCIAS (Colombia) Grant # 910–2015 -110171250457.

Data Availability The data that support the findings of this study are openly available. The reference is Cardenas-Sandoval, R. P. Effects of ultrasound stimuli on mechanical and biological properties of ligament fibroblasts. *Mendeley Data, v3* (2022). https://data.mendeley.com/datasets/mvwr8mjz3k. [Accessed 24 Nov 2022].

Declarations

Ethics Approval We obtained Lateral Collateral Ligaments (LCLs) from two male Wistar rats sacrificed in the animal research facility of the Pharmacy Faculty. They were sacrificed for exhibiting aggressive behavior. According to international regulations for laboratory animals, a zoologist specialist sacrificed the Wistar rats by using a faster CO_2 euthanasia method to decrease distress time. For this reason, an anesthetic protocol was unnecessary. After the research completion, it was not necessary to sacrifice other rats. Finally, the ethics committee of the Faculty of Sciences at the Universidad Nacional de Colombia (Protocol Number: FC-13–01082016) approved the research protocols.

Competing Interests The authors declare no competing interests.

References

1. Vicente-Manzanares M. Cell migration at a glance. J Cell Sci. 2005;118(21):4917–9.

2. Springer Nature. Cell migration. © Springer Nature Publishing, 2019.
3. William E. Prentice. Understanding and managing the healing process through rehabilitation. In: Hoogenboom B, Voight M, Prentice W, editors. Musculoskeletal Interventions: Techniques for Therapeutic Exercise. 3rd ed. New York: McGraw-Hill; 2013.
4. Nijenhuis N, Zhao X, Carisey A, Ballestrem C, Derby B. Combining AFM and acoustic probes to reveal changes in the elastic stiffness tensor of living cells. Biophys J. 2014;107(7):1502–12.
5. Nikolaev NI, Müller T, Williams DJ, Liu Y. Changes in the stiffness of human mesenchymal stem cells with the progress of cell death as measured by atomic force microscopy. Biomech. 2014;47(3):625–30.
6. Schulze KD, Zehnder SM, Urueña JM, Bhattacharjee T, Sawyer WG, Angelini TE. Elastic modulus and hydraulic permeability of MDCK monolayers. J Biomech. 2017;53:210–3.
7. Geltmeier A, Rinner B, Bade D, Meditz K, Witt R, Bicker U, et al. Characterization of dynamic behaviour of MCF7 and MCF10A cells in ultrasonic field using modal and harmonic analyses. PLoS One. 2015;10(8):1–20.
8. Shekofteh M, Mohseny M, Shahbodaghi A, Zayeri F, Rahimi F. The correlation among Y-index and other scientometric indicators. Curr Sci. 2016;110(9):1823–8.
9. Miller D, Smith N, Bailey M, Czarnota G, Hynynen K, Makin I. Overview of therapeutic ultrasound applications and safety considerations. J Ultrasound Med. 2012;31(4):623–34.
10. O'Brien WD Jr. Ultrasound-biophysics mechanisms. Prog Biophys Mol Biol. 2007;93(1–3):212–55.
11. Tole NM. Intensity of ultrasound. In: Ostensen H, editor. Basic physics of ultrasonographic imaging. Malta: World health organization; 2005. p. 33–4.
12. Rodríguez M. Ultrasonidos. In: Electroterapia en Fisioterapia. 2a ed. Buenos Aires: Editorial Médica Panamericana. 2004;515–51.
13. Khayamian MA, Baniassadi M, Abdolahad M. Monitoring the effect of sonoporation on the cells using electrochemical approach. Ultrason Sonochem. 2018;41:619–25. https://doi.org/10.1016/j.ultsonch.2017.10.030.
14. Paluch EK, Nelson CM, Biais N, Fabry B, Moeller J, Pruitt BL, et al. Mechanotransduction : use the force (s). BMC Biol. 2015;13(47):1–14.
15. Tsata V, Beis D. In full force. Mechanotransduction and morphogenesis during homeostasis and tissue regeneration. J Cardiovasc Dev Dis. 2020;7(40):1–18.
16. Herrmann H, Bär H, Kreplak L, Strelkov SV, Aebi U. Intermediate filaments: from cell architecture to nanomechanics. Nat Rev Mol Cell Biol. 2007;8(7):562–73.
17. Samandari M, Abrinia K, Mokhtari-Dizaji M, Tamayol A. Ultrasound induced strain cytoskeleton rearrangement: an experimental and simulation study. J Biomech. 2017;60:39–47.
18. Allsop G, Peckham M. Cytoskeleton and cell motility. Comprehensive Biotechnology, Second Edition. 2011;1:191–204.
19. Mizrahi N, Zhou EHH, Lenormand G, Krishnan R, Weihs D, Butler JP, et al. Low intensity ultrasound perturbs cytoskeleton dynamics. Soft Matter. 2012;8(8):2438–43.
20. Louw TM, Budhiraja G, Viljoen HJ, Subramanian A. Mechanotransduction of ultrasound is frequency dependent below the cavitation threshold. Ultrasound Med Biol. 2013;39(7):1303–19.
21. Alenghat FJ, Ingber DE. Mechanotransduction: all signals point to cytoskeleton, Matrix, and Integrins. Science's STKE. 2002;(119):pe6.
22. Tibbitt MW, Anseth KS. Dynamic microenvironments: the fourth dimension. Sci Transl Med. 2012;4(160):160 ps24 LP-160 ps24.
23. de Lucas B, Pérez LM, Bernal A, Gálvez BG. Ultrasound therapy: experiences and perspectives for regenerative medicine. Genes (Basel). 2020;11(9):1–21.
24. Tsai WC, Chen JYS, Pang JHS, Hsu CC, Lin MS, Chieh LW. Therapeutic ultrasound stimulation of tendon cell migration. Connect Tissue Res. 2008;49(5):367–73; http://www.tandfonline.com/doi/full/https://doi.org/10.1080/03008200802325359
25. Lennart DJ. Nonthermal effects of therapeutic ultrasound: the frequency resonance hypothesis. J Athl Train. 2002;37(3):293–9.
26. Lepeschkin WW, Goldman DE. Effects of ultrasound on cell structure. J Cell Physiol. 1952;40(3):383–97.
27. Iranmanesh I, Ohlin M, Ramachandraiah H, Ye S, Russom A, Wiklund M. Acoustic micro-vortexing of fluids, particles and cells in disposable microfluidic chips. Biomed Microdevices. 2016;18(4):1–7.
28. Carmine Pappalettere IM, Tachibana K. Effect of different ultrasound frequency sweep pattern on leukemic cells. In: Proceedings of the World Congress on Electrical Engineering and Computer Systems and Science (EECSS 2015). Barcelona. 2015;1–2.
29. Ivone M, Lamberti L, Pappalettere C, Caratozzolo MF, Tullo A. Experimental comparison Of MCF7 And MCF10A response to low intensity ultrasound. J Mech Med Biol. 2019;19(6):1–24.
30. Conneely M, Mcgloin D, Robertson P, Mclean WHI, Campbell PA. Influence of ultrasound exposure on cell-mechanical properties: a preliminary study on MCF7 human breast cancer cells. In: The 15th European Microscopy Congress. Manchester Central: J Microsc. 2012.
31. Izadifar Z, Babyn P, Chapman D. Mechanical and biological effects of ultrasound: a review of present knowledge. Ultrasound Med Biol. 2017;43(6):1085–104.
32. Rubin D, Anderton N, Smalberger C, Polliack J, Nathan M, Postema M. On the behaviour of living cells under the influence of ultrasound. Fluids. 2018;3(4):82.
33. Jiang YY, Park JK, Yoon HH, Choi H, Kim CW, Seo YK. Enhancing proliferation and ECM expression of human ACL fibroblasts by sonic vibration. Prep Biochem Biotechnol. 2015;45(5):476–90.
34. Oliveira PD de, Almeida Pires-Oliveira DA de, Dragonetti Bertin L, Fernandes Szezerbaty SK, Franco de Oliveira R. The effect of therapeutic ultrasound on fibroblast cells in vitro: the systematic review. Arch Med Deporte. 2018;35(183):50–5.
35. Henshaw DR, Attia E, Bhargava M, Hannafin JA. Canine ACL fibroblast integrin expression and cell alignment in response to cyclic tensile strain in three-dimensional. J Orthop Res. 2006;24(3):481–90.
36. Spitalnik P. Histology laboratory manual 2015–2016. College of Physicians and Surgeons: Columbia University; 2015.
37. Karlsson LK, Junker JPE, Grenegård M, Kratz G. Human dermal fibroblasts: a potential cell source for endothelialization of vascular grafts. Ann Vasc Surg. 2009;23(5):663–74.
38. Abercrombie M. Fibroblasts. J Clin Pathol. 1978;12:1–6.
39. Uhlemann C, Heinig B, Wollina U. Therapeutic ultrasound in lower extremity wound management. Int J Low Extrem Wounds. 2003;2(3):152–7.
40. Ng COY, Ng GYF, See EKN, Leung MCP. Therapeutic ultrasound improves strength of achilles tendon repair in rats. Ultrasound Med Biol. 2003;29(10):1501–6.
41. Robertson VJ, Baker KG. A review of therapeutic ultrasound: effectiveness studies. Phys Ther. 2001;81:1339–50.
42. Dr. R, Dr. Jibi P, Dr. Hepsibah S, Dr. Sathya P. Effect of ultrasound therapy and cryotherapy over taping technique in patients with acute lateral ankle sprain. Int J Pharma Bio Sci. 2021;11(4):9–15.
43. Harle J, Salih V, Mayia F, Knowles J, Olsen I. Effects of ultrasound on the growth and function of bone and periodontal ligament cells in vitro. Ultrasound Med Biol. 2001Apr;27(4):579–86.
44. Carrer V de M, Setti JAP, Veronez D da L, Moser AD. Continuous therapeutic ultrasound in the healing process in rat skin. Fisioterapia em Movimento. 2015;28(4):751–8.
45. Warden SJ, Avin KG, Beck EM, DeWolf ME, Hagemeier MA, Martin KM. Low-intensity pulsed ultrasound accelerates and a

nonsteroidal anti-inflammatory drug delays knee ligament healing. Am J Sports Med. 2006;34(7):1094–102.
46. Chen J. Nanobiomechanics of living cells: a review. Interface Focus. 2014;4(2):20130055–20130055.
47. Solon J, Levental I, Sengupta K, Georges PC, Janmey PA. Fibroblast adaptation and stiffness matching to soft elastic substrates. Biophys J. 2007;93(12):4453–61.
48. Managuli V, Roy S. Asymptotical correction to bottom substrate effect arising in AFM indentation of thin samples and adherent cells using conical tips. Exp Mech. 2018;1–9.
49. Pegoraro AF, Janmey P, Weitz DA. Mechanical properties of the cytoskeleton and cells. Cold Spring Harb Perspect Biol. 2017;9(11).
50. Barreto S, Lacroix D. Quantification of CSK mechanics and deformation in relation to cellular functioning. In: Multiscale Mechanobiology in Tissue Engineering. Singapore: Springer Singapore; 2019;181–93.
51. Ingber DE, Tensegrity I. Cell structure and hierarchical systems biology. J Cell Sci. 2003;116(7):1157–73.
52. Hoh JH, Schoenenberger C a. Surface morphology and mechanical properties of MDCK monolayers by atomic force microscopy. J Cell Sci. 1994;107(Pt 5):1105–14.
53. Jacobs CR, Huang H, Kwon RY. Introduction to cell mechanics and mechanobiology. 1st ed. New York: Garland Science; 2012. p. 350.
54. Ofek G, Wiltz DC, Athanasiou KA. Contribution of the cytoskeleton to the compressive properties and recovery behavior of single cells. Biophys J. 2009;97(7):1873–82.
55. Guilak F, Haider MA, Setton LA, Laursen TodA, Baaijens FPT. Multiphasic models of cell mechanics Farshid. In: Mofrad MRK, Kamm RD, editors. Cytoskeletal mechanics Models and measurements. New York: Cambridge University Press; 2006;256.
56. Mcgarry JG, Prendergast PJ. A three-dimensional finite element model of an adherent eukaryotic cell. Eur Cells Mater. 2004;7:27–34.
57. Palmer JS, Boyce MC. Constitutive modeling of the stress–strain behavior of F-actin filament networks. Acta Biomater. 2008;4:597–612.
58. Unterberger MJ, Schmoller KM, Bausch AR, Holzapfel GA. A new approach to model cross-linked actin networks: multi-scale continuum formulation and computational analysis. J Mech Behav Biomed Mater. 2013;1(22):95–114.
59. Ananthakrishnan R, Guck J, Wottawah F, Schinkinger S, Lincoln B, Romeyke M, et al. Quantifying the contribution of actin networks to the elastic strength of fibroblasts. J Theor Biol. 2006;242:502–16.
60. Hoyle NP, Seinkmane E, Putker M, Feeney KA, Krogager TP, Chesham JE, et al. Circadian actin dynamics drive rhythmic fibroblast mobilization during wound healing. Sci Transl Med. 2017;9(415):1–10.
61. Chen T jung, Wu C ching, Tang M jer, Huang J shin, Su F chin. Complexity of the tensegrity structure for dynamic energy and force distribution of cytoskeleton during cell spreading. PLoS One. 2010;5(12):1–11.
62. Pastrana HF, Cartagena-Rivera AX, Raman A, Ávila A. Evaluation of the elastic Young's modulus and cytotoxicity variations in fibroblasts exposed to carbon-based nanomaterials. J Nanobiotechnology. 2019;17(1):1–15.
63. Bergman E, Goldbart R, Traitel T, Amar-Lewis E, Zorea J, Yegodayev K, et al. Cell stiffness predicts cancer cell sensitivity to ultrasound as a selective superficial cancer therapy. Bioeng Transl Med. 2021;6(3):1–13.
64. Efremov YM, Shpichka AI, Kotova SL, Timashev PS. Viscoelastic mapping of cells based on fast force volume and PeakForce Tapping. Soft Matter. 2019;15(27):5455–63.
65. Guz N, Dokukin M, Kalaparthi V, Sokolov I. If cell mechanics can be described by elastic modulus: study of different models and probes used in indentation experiments. Biophys J. 2014;107(3):564–75.
66. Jaganathan, Saravana Kumar Subramanian AP, Vellayappan MV, Balaji A, Aruna John A, Jaganathan AK, Supriyanto E. Natural frequency of cancer cells as a starting point in cancer treatment. Curr Sci. 2016;110(9):1828–32.
67. Tsaklis PV. Presentation of acoustic waves propagation and their effects through human body tissues. Human Movement. 2010;11(1):58–65.
68. Robertson VJ, Ward AR. Limited interchangeability of methods of applying 1 MHz ultrasound. Arch Phys Med Rehabil. 1996;77(4):379–84; http://www.ncbi.nlm.nih.gov/pubmed/8607763
69. Ivone M, Pappalettere C, Watanabe A, Tachibana K. Study of cellular response induced by low intensity ultrasound frequency sweep pattern on myelomonocytic lymphoma U937 cells. J Ultrasound;19(3):167–74; http://link.springer.com/https://doi.org/10.1007/s40477-016-0199-0. Accessed 7 Nov 2019.
70. Wang P, Leung AW, Xu C. Low-intensity ultrasound-induced cellular destruction and autophagy of nasopharyngeal carcinoma cells. Exp Ther Med. 2011;2(5):849–52.
71. Bertin LD, Poli-Frederico RC, Pires Oliveira DAA, Oliveira PD, Pires FB, Silva AFS, et al. Analysis of cell viability and gene expression after continuous ultrasound therapy in L929 fibroblast cells. Am J Phys Med Rehabil. 2019;98(5):369–72.
72. Zhang C, Li J, Zhang L, Zhou Y, Hou W, Quan H, et al. Effects of mechanical vibration on proliferation and osteogenic differentiation of human periodontal ligament stem cells. Arch Oral Biol;57(10):1395–407; http://www.ncbi.nlm.nih.gov/pubmed/22595622. Accessed 27 Feb 2020.
73. De OPD, Oliveira DAAP, Martinago CC, Célia R, Frederico P, Soares CP, et al. Effect of low-intensity pulsed ultrasound therapy on a fibroblasts cell culture. Fisioterapia e Pesquisa. 2015;22(2):112–8.
74. Bohari SP, Grover LM, Hukins DW. Pulsed low-intensity ultrasound increases proliferation and extracelluar matrix production by human dermal fibroblasts in three-dimensional culture. J Tissue Eng. 2015;6:2041731415615777.
75. Hormozi-Moghaddam Z, Mokhtari-Dizaji M, Nilforoshzadeh MA, Bakhshandeh M. Low-intensity ultrasound to induce proliferation and collagen I expression of adipose-derived mesenchymal stem cells and fibroblast cells in co-culture. Measurement (Lond). 2021;167(May 2020):108280.
76. Yadav K, Singhal N, Rishi V, Yadav H. Cell proliferation assays. eLS John Wiley & Sons, Ltd: Chichester. 2014;
77. Doan N, Reher P, Meghji S, Harris M. In vitro effects of therapeutic ultrasound on cell proliferation, protein synthesis, and cytokine production by human fibroblasts, osteoblasts, and monocytes. J Oral Maxillofac Surg. 1999;57(4):409–19.
78. de Oliveira Perrucini PD, Poli-Frederico RC, de Almeida Pires-Oliveira DA, Dragonetti Bertin L, Beltrão Pires F, Shimoya-Bittencourt W, et al. Anti-inflammatory and healing effects of pulsed ultrasound therapy on fibroblasts. Am J Phys Med Rehabil. 2020;99(1):19–25.
79. Man J, Shelton RM, Cooper PR, Landini G, Scheven B a. Low intensity ultrasound stimulates osteoblast migration at different frequencies. J Bone Miner Metab. 2012;30(5):602–7.
80. Atherton P, Lausecker F, Harrison A, Ballestrem C. Low-intensity pulsed ultrasound promotes cell motility through vinculin-controlled Rac1 GTPase activity. J Cell Sci. 2017;130(14):2277–91.
81. Leng X, Shang J, Gao D, Wu J. Low-intensity pulsed ultrasound promotes proliferation and migration of HaCaT keratinocytes through the PI3K / AKT and JNK pathways. Braz J Med Biol Res. 2018;51(12):1–8.
82. Kuivaniemi H, Tromp G. Type III collagen (COL3A1): Gene and protein structure, tissue distribution, and associated diseases. Gene. 2020;707:151–71.
83. Tsai WC, Pang JHS, Hsu CC, Chu NK, Lin MS, Hu CF. Ultrasound stimulation of types I and III collagen expression of tendon

cell and upregulation of transforming growth factor b. J Orthop Res. 2006;24:1310–6.
84. Lee JY, Min DJ, Kim W, Bin BH, Kim K, Cho EG. Non pharmacological high-intensity ultrasound treatment of human dermal fibroblasts to accelerate wound healing. Sci Rep. 2021;11(1).
85. Thoumine O, Meister JJ. Dynamics of adhesive rupture between fibroblasts and fibronectin: microplate manipulations and deterministic model. Eur Biophys J. 2000;29(6):409–19.
86. Hurtley SM. Cell Biology of the Cytoskeleton. Science (1979). 1998;279(5350):459.
87. Qin Z, Fisher GJ, Voorhees JJ, Quan T. Actin cytoskeleton assembly regulates collagen production via TGF-β type II receptor in human skin fibroblasts. J Cell Mol Med. 2018;22(9):4085–96.
88. Atherton P, Lausecker F, Harrison A, Ballestrem C. Low-intensity pulsed ultrasound promotes cell motility through vinculin-controlled Rac1 GTPase activity. J Cell Sci. 2017;130(14):2277–91; http://jcs.biologists.org/lookup/doi/https://doi.org/10.1242/jcs.192781
89. Wang YL. Reorganization of actin filament bundles in living fibroblasts. J Cell Biol. 1984;99(4 I):1478–85.
90. Karna E, Szoka L, Huynh TYL, Palka JA. Proline-dependent regulation of collagen metabolism. Cell Mol Life Sci. 2020;77(10):1911–8. https://doi.org/10.1007/s00018-019-03363-3.